EUROGRAPHICS 2013 / I. Navazo, P. Poulin
(Guest Editors)

Volume 32 (2013), Number 2

Stylized and Performative Gaze for Character Animation

Tomislav Pejsa, Bilge Mutlu, and Michael Gleicher

University of Wisconsin–Madison

Abstract

Existing models of gaze motion for character animation simulate human movements, incorporating anatomical, neurophysiological, and functional constraints. While these models enable the synthesis of humanlike gaze motion, they only do so in characters that conform to human anatomical proportions, causing undesirable artifacts such as cross-eyedness in characters with non-human or exaggerated human geometry. In this paper, we extend a state-of-the-art parametric model of human gaze motion with control parameters for specifying character geometry, gaze dynamics, and performative characteristics in order to create an enhanced model that supports gaze motion in characters with a wide range of geometric properties that is free of these artifacts. The model also affords "staging effects" by offering softer functional constraints and more control over the appearance of the character's gaze movements. An evaluation study showed that the model, compared with the state-of-the-art model, creates gaze motion with fewer artifacts in characters with non-human or exaggerated human geometry while retaining their naturalness and communicative accuracy.

Categories and Subject Descriptors (according to ACM CCS): I.3.7 [Computer Graphics]: Animation—

1. Introduction

Gaze shifts are movements of the eyes and the head that redirect the gaze of a source toward a specific target. Animating gaze shifts for virtual humans often involves the use of parametric models of human gaze behavior. While these models enable virtual humans to perform natural and accurate gaze shifts, their use involves two key challenges. First, to capture the subtlety, richness, and expression of these movements, state-of-the-art models (e.g., [APMG12b, LM10]) incorporate anatomic and neurophysiological constraints as well as functional requirements. While these constraints enable characters that conform to the proportions of human anatomy to achieve humanlike gaze motion, they limit the applicability of these models to non-human or stylized characters. Such characters have exaggerated geometry with large and often asymmetrically shaped eyes such as those illustrated in Figure 1. Applying models of realistic human gaze motion to such characters can magnify or distort elements of gaze mechanics and potentially lead to anomalous poses and movements such as noticeable cross-eyedness or disconjugate eye movements. These phenomena can appear unpleasant and alter what these movements communicate.

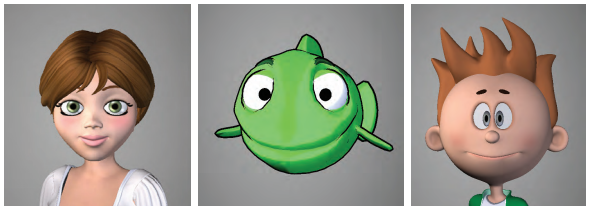

Figure 1: *Examples of stylized characters. Characters 1 and 2 have large eyes and high inter-eye distance. Characters 2 and 3 have asymmetric eye motor range (OMR). Character 3 has narrow OMR and low inter-eye distance.*

Second, existing models seek to conform to functional constraints; the eyes must align with their target so that the character can see it. However, this requirement does not exist in theater, film, and cartoon animation, where the primary purpose of gaze shifts is to communicate ideas to the audience. For example, a stage actor does not need to physically align his eyes with an object of interest but merely needs to gaze toward the object's general direction to communicate his interest. Existing models lack support for animating such performative gaze behaviors.

To address these challenges, we present a model for *stylized* and *performative* gaze shifts that enhances a state-of-the-art model by relaxing model constraints in order to provide greater parametric control and applicability to a wider

© 2013 The Author(s)
Computer Graphics Forum © 2013 The Eurographics Association and Blackwell Publishing Ltd. Published by Blackwell Publishing, 9600 Garsington Road, Oxford OX4 2DQ, UK and 350 Main Street, Malden, MA 02148, USA.

range of character designs. Stylized gaze shifts are enabled by a set of parameters for character geometry (e.g., eye size and motor range) that adapt the target pose and gaze shift dynamics to the character's specific features. These extensions are designed to remain as faithful as possible to the human model while reducing undesirable artifacts.

Our model supports *performative* gaze by relaxing the functional requirements and allowing explicit control over the degree of alignment with the viewer toward achieving greater social expressivity [AC76, GKC69, APMG12a]. The model also integrates *view dependence*, which purposefully alters gaze direction (e.g., to remove cross-eyedness or achieve more alignment with the viewer) under the assumption that these alterations will not impair the viewer's perception of gaze direction. Prior studies of gaze indicate that observers can accurately identify face-directed gaze when the gaze source is facing them and otherwise use rough estimates of gaze direction based on head orientation [CE73]. Informed by these findings, view dependency enables more flexible transformations of gaze direction when the character does not gaze directly at the viewer.

In order to animate gaze shifts in characters with a broader range of geometric properties while reducing artifacts and supporting performative gaze motion, our model departs from a validated model of human gaze behavior. An evaluation of the model confirms that it significantly reduces the frequency and severity of gaze artifacts across a wide range of characters and maintains the perceived naturalness and communicative accuracy of the state-of-the-art model.

The main contribution of this paper is a model for gaze shifts that applies to a wide range of characters and allows for performative effects. Specific contributions include:

- Identification of undesirable visual artifacts of models for human gaze behavior on stylized characters.
- A model that incorporates parameters for character geometry and gaze dynamics into a model of human gaze behavior and allows animation of gaze motion for stylized characters with reduced visual artifacts.
- An explicit consideration of performative gaze as part of a model, relaxing functional constraints where appropriate.

2. Related Work

Existing models of gaze can be classified as data-driven or procedural. Data-driven models rely on motion capture data to synthesize natural-looking gaze behaviors. Examples of this approach include the *Expressive Gaze Model* [LM10], a model parameterized by emotion that uses a motion warping approach to animate the eyes and head. Other examples seek to capture non-deterministic correlations between gaze, eye blinks, and head motion [DLN05], use motion-capture poses to animate gaze shifts that engage the entire upper body [Hec07], or incorporate neurobiological models of visual attention [IDP06].

Our model falls into the category of procedural gaze models. These models do not rely on motion capture data and typically offer a greater degree of parametric control. The procedural model proposed by Andrist et al. [APMG12b] offers fine parametric control over head-eye coordination to target specific communicative effects. Similarly, the head propensity model proposed by Peters and Qureshi [PQ10] provides parameters for specifying how much the head contributes to the gaze shift. Li et al. [LML09] have developed an emotion-based model that includes eye blinks and pupil dilation. The *Rickel Gaze Model* [LMT*07] specifies a set of cognitive states that trigger appropriate gaze shifts. The attention-based model proposed by Grillon et al. [GT09] computes likely points of interest given current character motion. Finally, a number of models specify composite gaze behaviors in specific contexts such as idle gaze in conversations [LBB02, KB01, GB06] and in public [CGV09]. However, these models do not explicitly consider animation of stylized characters or performative aspects of gaze.

3. Visual Artifacts in Gaze

State-of-the-art models for gaze shifts incorporate features of human anatomy, including eye dimensions, inter-eye distance, and symmetry of oculomotor range. When such models are applied to a stylized character with exaggerated or non-human anatomic features, we observe two kinds of phenomena. First, anatomically correct, but rarely observed, elements of human gaze can be magnified and become noticeable. Second, asymmetry and exaggerated size of the eyes can cause anomalous situations that are rare or impossible in healthy human gaze. We argue that these phenomena are undesirable, as they can distract the viewer and/or alter the semantics of the gaze shift. Below, we catalog specific visual artifacts that our gaze model seeks to address.

Cross-eyedness – Cross-eyedness occurs when the eyes significantly angle inward (towards each other). In humans, while convergence on a target necessitate some amount of inward angle, excessive amounts are straining to maintain. Small amounts of cross-eyedness are not noticeable due to the small size of the eyes, and larger amounts are caused by unnatural viewing conditions or an explicit expression. In

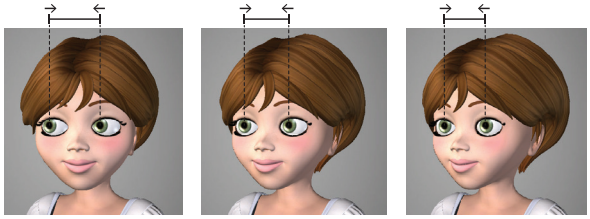

Figure 2: *Eye retraction example. The right eye has aligned with the target and is retracting as the left eye moves forward. Notation: Solid line indicates inter-eye distance. Arrows → and ← indicate eye movement direction.*

© 2013 The Author(s)
© 2013 The Eurographics Association and Blackwell Publishing Ltd.

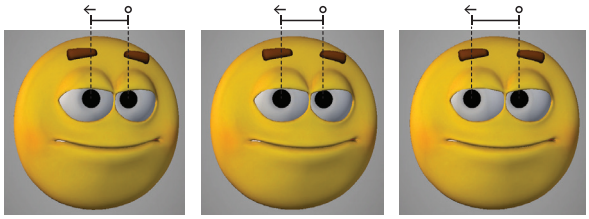

Figure 3: *Stuck eye example. The right eye is moving ahead, while the left eye is blocked by OMR. Notation: Dot ∘ indicates that the eye is stationary.*

characters with large or widely spaced eyes, cross-eyedness becomes noticeable even in more standard viewing (Figure 7).

Speedy eyes – Human eyes have low mass and strong muscles that support fast and abrupt movements. In characters with larger eyes, such movements can appear implausible.

OMR-block – When the eyes initiate a gaze shift and reach the boundary of the *ocular motor range* (OMR), they are effectively blocked in their movements until the head brings them into alignment with the gaze target. While natural and common in humans, this phenomenon can appear anomalous in stylized characters; during this prolonged phase when the eyes are unable to move, the character may appear static and puppet-like. We believe this phenomenon to be caused by *speedy eyes*; the eyes cover the distance between starting position and OMR in an unrealistic speed, resulting in an unusually long period of OMR-block. The visual artifact becomes even more prevalent with narrow OMR, a common property of stylized characters.

Eye retraction – In human gaze, when the head brings the eyes into alignment with the gaze target, the *vestibulo-ocular reflex* (VOR) effectively locks the eyes onto the target as the head catches up, rotating the eyes in the opposite direction of the head movement. While this standard feature of human gaze does not appear as anomalous in real humans or characters with humanlike proportions, in stylized characters with large eyes, it can appear as if the eyes have overshot the target and are now suddenly retracting in order to realign with it (Figure 2). We believe that the cause of this illusion is excessive eye velocities that cause the eyes to advance further ahead and retract more than expected.

Stuck eye – Stuck eye is caused by asymmetry of eye shape, which necessarily involves asymmetry in the OMR. The leading eye in the gaze shift, which rotates outward, has a greater distance to cover before reaching OMR than the trailing eye. However, when both eyes move at the same velocity, as is the case with human eyes, the trailing eye will reach its OMR boundary sooner and become blocked, while the other eye will continue moving (Figure 3). Movement in one eye does not occur in human gaze except in medical conditions such as amblyopia and therefore can appear abnormal.

Eye divergence – When the eyes have asymmetric OMR, their gaze directions can become divergent as they reach their respective OMR boundaries. Although difficult to observe in static poses, this divergence might cause disconjugate eye movements and appear jarring when the eyes are brought into alignment with the gaze target. In these movements, the leading eye will reach the gaze target before the trailing eye, and VOR causes the eye to rotate backward, while the trailing eye is still moving forward (Figure 8). Such divergent orientations and movements are improbable in healthy human gaze and appear anomalous.

4. Stylized and Performative Gaze Shifts

The visual artifacts described in the previous section occur because human gaze mechanics do not necessarily apply to non-human characters. To create a model that can be applied more broadly, we extend an existing model of human gaze, under the premise that we want to retain as much of the human behavior as possible. In this work, we build on the model for gaze shifts proposed by Andrist et al. [APMG12b], which we hereafter refer to as the *baseline* gaze model, as a state-of-the-art model of gaze that has been validated in previous studies [APMG12b, APMG12a] and shown to achieve significant communicative effects.

4.1. Baseline Model

Figure 4 provides an overview of gaze shifts generated by the baseline model. Before the gaze shift begins, the model is provided with a set of parameters, including gaze target position T and head alignment α_H. Head alignment specifies how much the head should align with the gaze target; it ranges from 0 (using minimal head motion) to 1 (fully align the head with the target). At the start of the gaze shift (A), eyes and head begin rotating toward the target together. Since eyes move much faster than the head does, they quickly get ahead and reach their OMR (B), where they remain blocked as the head catches up. Eventually the head rotates far enough to bring the eyes into alignment with the target (C). VOR locks the eyes onto the target as the head catches up. Depending on the specified head alignment, the head will either stop moving immediately or continue rotating until it reaches the required alignment with the target (D). For further details of the model, please see [APMG12b].

When the eyes are moving freely (phase A to B), their motion is governed by the velocity profile shown in Figure 5. A very similar profile is also used for head motion. Peak velocity V_{MAX} in the profile is not constant and is instead computed at the start of every gaze shift based on the magnitude of the upcoming eye movement, according to the following formula:

$$\begin{aligned} V_{MAX} &= (\frac{2}{75}A_{MIN} + \frac{1}{6})V_0 \\ A_{MIN} &= min(\min_{j \in Eyes}(D_j), OMR) \end{aligned} \quad (1)$$

© 2013 The Author(s)
© 2013 The Eurographics Association and Blackwell Publishing Ltd.

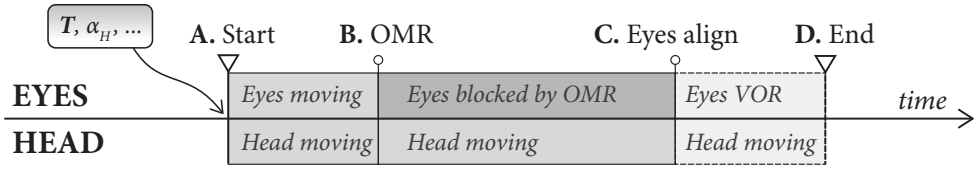

Figure 4: *Gaze shift phases in the baseline gaze model.*

where D_j is rotational distance (in degrees) that the eye j has to rotate before reaching the target. V_0 is a user-specifiable velocity parameter, normally left at the default value of $150 deg/s$.

The gaze model also features a model of eye blinks that probabilistically generates idle blinks at a constant average rate and gaze-evoked blinks that occur during the gaze shift based on the model originally described in [PQ10]. Evinger et al. [EMP*94] hypothesize the purpose of gaze-evoked eye blinks is to protect the eye during the movement and lubricate the cornea.

4.2. Gaze Shifts for Stylized Characters

In consideration of the challenges associated with applying a model of human gaze behavior to stylized or non-human characters, we extend the model above with parameters that account for the non-realistic anatomy of the latter and techniques to explicitly avoid the artifacts described in the previous section, while seeking to maintain as much of the human movement as possible. Our extensions fall into three categories. First, we introduce changes to how the target pose of the eyes and head is computed in order to prevent the occurrence of anomalous poses. Second, we extend the computation of eye movement dynamics to account for variable physical constraints of the exaggerated geometries that are common in stylized characters. Third, we manipulate the timings of gaze-evoked eye blinks to co-occur with potential visual artifacts to conceal them.

To specify the character's specific properties, we introduce four designer-adjustable parameters to the model. Eye width, W, is the width of the eye as a factor of the width of the typical human eye (approximately $2.5cm$), ranging from 1 to 3 in the characters we encountered. Eye strength F allows for tuning the strength of the character's eye muscles relative to that of a human. Additionally, we replace the single parameter of the *OMR* in humans with parameters OMR_{IN} and OMR_{OUT} that afford asymmetric eye motion by specifying the inward and outward OMR limits (in angle degrees), respectively. Eye width, W, and OMR parameters, OMR_{IN} and OMR_{OUT}, can be determined from face geometry, while we use the value of $W^3/3$ for eye strength, F, which works well across a range of characters.

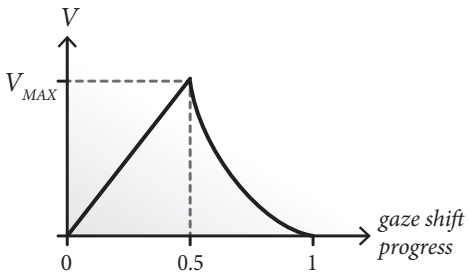

Figure 5: *Velocity profile governing eye movements. Eyes accelerate until they reach peak velocity v_{MAX} halfway through the gaze shift and then decelerate until the end of the gaze shift.*

4.2.1. Target Pose Adaptation

The baseline model, when applied to a stylized character with large eyes, is prone to bring the eyes into a noticeably cross-eyed state. If the character's eyes are asymmetric, then the eyes can also be led into a divergent state, which will become noticeable as the leading eye reaches the gaze target and VOR reverses its direction of movement. To avoid these artifacts, our model adapts the target pose of the eyes and head at the beginning of the gaze shift by adjusting effective gaze target position and OMR parameters.

Cross-eyedness Removal – Our approach to remove cross-eyedness is illustrated in Figure 6. We measure cross-eyedness as the angle between the gaze directions of the two eyes, γ. Allowable cross-eyedness is defined by a threshold γ_{MAX}, which we leave at a default value of 0.002° for the examples in this paper. We define the *effective target position* as the position behind the physical gaze target that the eyes can converge on without violating the cross-eyedness threshold. It is calculated by moving the target position away from

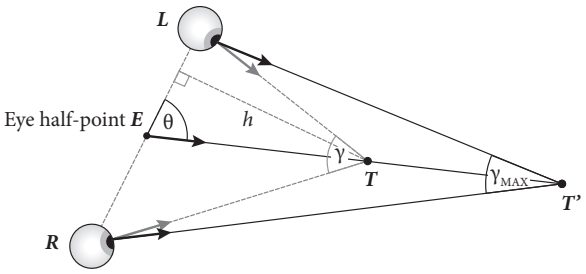

Figure 6: *Our approach to reducing cross-eyedness in the target gaze pose.*

© 2013 The Author(s)
© 2013 The Eurographics Association and Blackwell Publishing Ltd.

Figure 7: *Cross-eyedness and its reduction. Left: Cross-eyed character. Right: Cross-eyedness reduced by our model.*

the character to reduce γ below the threshold value γ_{MAX},

$$T' = E + \frac{T-E}{||T-E||}\frac{\sin(\theta+\gamma_{MAX}/2)}{sin(\gamma_{MAX}/2)}||L-E||. \quad (2)$$

The above technique is effective at reducing cross-eyedness as shown in Figure 7.

The cross-eyedness removal technique is applied in a view-dependent manner; we may only apply it if the viewer cannot notice it from the current viewpoint.

If the viewer is the gaze target, they may notice the character is looking a bit "past" them if cross-eyedness removal is applied. Therefore, the cross-eyedness threshold γ_{MAX} is adjusted based on the target viewing angle ϕ_T, which we define as the angle between the viewer's gaze direction and the character's gaze direction at the target pose. γ_{MAX} is adjusted as follows:

$$\begin{aligned} \gamma'_{MAX} &= 2OMR_{IN} + (\gamma_{MAX} - 2OMR_{IN})p_\phi \quad (3) \\ p_\phi &= \phi_T/(9.6W),\ 0 \leq t \leq 1 \end{aligned}$$

where OMR_{IN} is inward OMR of the eye, and W is the eye width parameter. The 9.6° constant is derived from parameters of the viewing cone in which humans are able to detect subtle differences in gaze direction [AC76]. We scale this value by W, as larger eyes may make such judgements easier. The viewing cone parameter, p_ϕ, expresses the drop-off

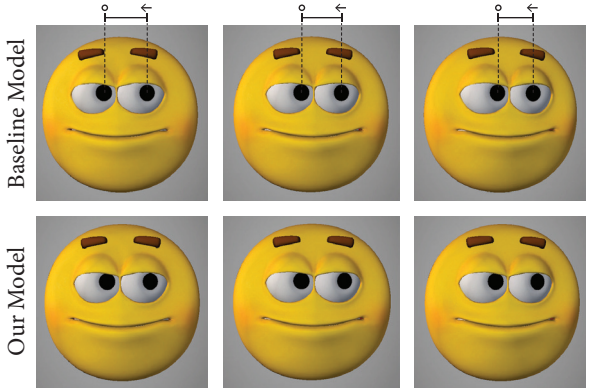

Figure 8: *Example of eye divergence handling. Top: VOR begins to move the left eye immediately on alignment. Bottom: Our model ensures that VOR begins eye movement only after the right eye has aligned.*

in judgement accuracy from the center of the cone towards the edge. We use p_ϕ to vary allowable cross-eyedness from the mechanical limit, $2OMR_{IN}$, at the center to γ_{MAX} at the cone's edge and beyond.

Eye Divergence – A consequence of OMR asymmetry, eye divergence is handled by allowing the eyes to diverge during the gaze shift and imposing the principle that VOR for both eyes must trigger *at the same time*. The leading eye will always overshoot the gaze target by a small amount and only begin moving in the opposite direction (due to VOR) when the trailing eye has reached the target. This behavior prevents the leading eye from aligning exactly with the target, as the accumulated overshoot rotation introduces an offset into the eye's target rotation. However, much like with cross-eyedness removal, this minor deviation from correct gaze convergence is difficult to detect. This technique is therefore an effective way of eliminating disconjugate eye movements as shown in Figure 8.

As with cross-eyedness removal, eye divergence is applied in a view-dependent manner. The target overshoot introduced by the technique may be noticeable to the viewer at very low viewing angles, which we therefore adjust using the viewing cone parameter, p_ϕ, that we defined in the previous subsection. Specifically, we scale the outward OMR based on target viewing angle, ϕ_T,

$$OMR'_{OUT} = OMR_{IN} + (OMR_{OUT} - OMR_{IN})p_\phi \quad (4)$$

This adjustment ensures that outward OMR will contract at low ϕ_T, making the OMR symmetrical.

4.2.2. Gaze Dynamics

Because most stylized characters do not have the same proportions and oculomotor constraints as humans, our model includes specific extensions to the baseline model to consider the additional character parameters described above to compute its dynamics. To preserve the characteristics of the movement, the model uses the velocity profile in Figure 5 but changes the manner in which V_{MAX} is computed by defining peak velocities, $V_{MAX,j}$, for each eye, departing from the assumption that both eyes have the same peak velocity. It uses eye width, W, and muscle strength, F, to compute these velocities. As volume—and therefore mass—increases with W^3, peak velocity is scaled down by the same factor. F is used to compute an intermediate parameter F', which varies depending on how much the head contributes to the gaze shift. We compute F' as follows:

$$F' = (1-\alpha_H)W^3 + \alpha_H F. \quad (5)$$

The parameter α_H specifies how much the head contributes to the gaze shift. When the head carries the eyes

© 2013 The Author(s)
© 2013 The Eurographics Association and Blackwell Publishing Ltd.

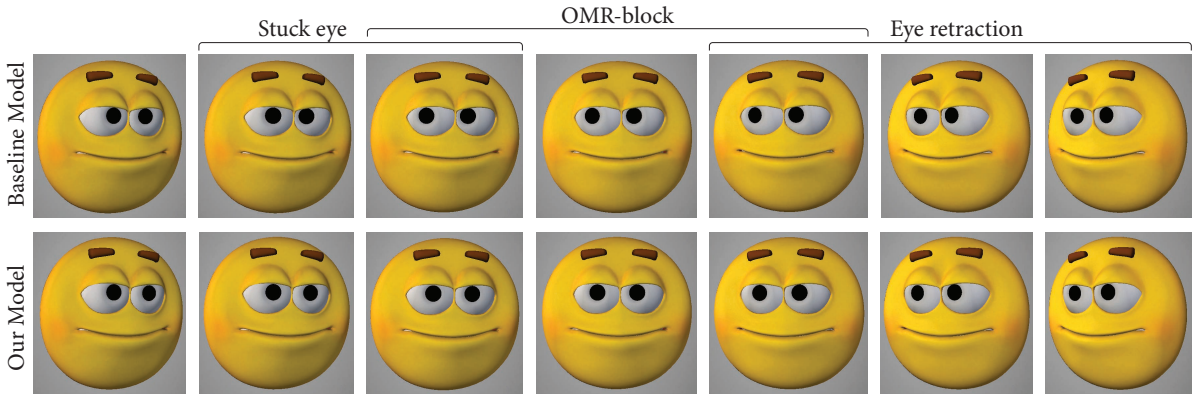

Figure 9: *Gaze shifts with different gaze dynamics. Top: Baseline model. The gaze shift contains the artifacts stuck eye, OMR-block, and eye retraction. Bottom: Our model. The artifacts of the baseline model are reduced.*

through most of the gaze shift (high α_H), eye velocity should be lower in order to prevent the eyes from appearing improbably fast. When the head moves only a small distance, the eyes should move more quickly to prevent the gaze shift from appearing slow and sluggish.

Our method must also account for OMR asymmetry to prevent artifacts such as *stuck eye* from occurring. Assume that $D_{OMR,j}$ is the distance that eye j can rotate before reaching OMR, while A_{MAX} is the highest rotational distance to OMR for each eye. The peak velocity is scaled by $D_{OMR,j}/A_{MAX}$ to slow down the eye that has less rotation to complete, thus ensuring that both eyes reach OMR at the same time.

Finally, we introduce a velocity multiplier parameter, χ, and apply it uniformly to eye and head velocities in order to make the character's gaze appear livelier or more expressive and to better reflect their personality and mood. By default, χ is set to 1, although we use values between 1.2 and 1.7 for our stylized characters.

We introduce these modifications to Equation 1 to create the following updated equation for calculating peak velocity:

$$V_{MAX,j} = \frac{F}{W^3}\left(\frac{2}{75}A_{MAX} + \frac{1}{6}\right)\frac{D_{OMR}}{A_{MAX}}\chi V_0 \qquad (6)$$

The first, third, and fourth terms implement our modifications to gaze dynamics. The second term speeds up or slows down the eyes depending on eye movement distance and is similar to the term used by the baseline model to calculate peak velocity, except that A_{MIN} is replaced by A_{MAX}.

Using the above method of calculating peak velocity reduces artifacts related to gaze dynamics, producing gaze shifts that appear smoother and more lifelike. The stuck eye artifact is largely eliminated; the amount of time spent in the state of OMR-block is greatly reduced; and VOR causes less eye retraction (Figure 9). The eye retraction cannot be completely eliminated, as some VOR must occur to achieve the specified head alignment and thus produce desired communicative effects.

4.2.3. Gaze-evoked Eye Blinks

As described in section 4.1, the baseline gaze model also incorporates an ancillary model of gaze-evoked eye blinks. The model probabilistically determines whether or not a gaze-evoked eye blink will occur at the beginning of the gaze shift. In humans, eye blinks can occur at any point during the gaze shift. Our model uses this flexibility to time gaze-evoked eye blinks to co-occur with potential eye retraction artifacts to conceal them (Figure 10).

Our implementation generates a gaze-evoked eye blink at the start of the gaze shift, using the same probabilistic method as in the baseline model. However, when determining the timing of the blink, it considers estimates of the duration of the VOR phase of the gaze shift, T_{VOR}, and the time when VOR phase will begin, t_{VOR}. If T_{VOR} is greater than a threshold value, then the gaze-evoked blink is scheduled to begin at $t_{VOR} - 0.35T_B$, where T_B is a probabilistically generated blink duration, and $0.35T_B$ is the time when eyes are fully closed.

Figure 10: *A gaze-evoked eye blink during the VOR phase. The blink conceals the retraction in the left eye.*

© 2013 The Author(s)
© 2013 The Eurographics Association and Blackwell Publishing Ltd.

4.3. Performative Gaze Shifts

While humans use gaze primarily to direct their attention to or seek information from their environment, in acting and cartoon animation, these primary goals are replaced by communicating ideas to and creating engagement with an audience. These goals are achieved by performing partial gaze shifts in the general direction of the object of interest and/or attention in order to convey the idea that the character is looking at the object without precisely aligning gaze with it. This performative behavior allows the character to retain partial alignment with the audience, which recent research has shown to improve how the viewer evaluates the character in measures such as engagement, likability, and trustworthiness [APMG12a].

Our model provides explicit support for partial gaze shifts by exposing the eye alignment parameter, α_E, which allows the designer to specify the desired amount of alignment with the target. An α_E of 1 causes the eyes to fully align with the target in a way that is similar to human gaze. We find that values between 0.6 and 1 produce good performative effects. With parameter values smaller than 1, the character will gaze toward a point directly between the gaze target and the viewer, which we call the *effective gaze target*. In order to convince the viewer that the character is gazing toward the real target, the two targets must occupy the same screen-space position, as illustrated in Figure 11.

Figure 12 illustrates how correct partial eye alignment is achieved. We compute the intermediate rotation of each eye, E, using $q_I = slerp(q_S, q_T, \alpha_E)$, where q_S and q_T are eye rotations in the source and target pose, respectively. At this rotation, gaze direction is given by vector $\mathbf{e_I}$. The view direction, $\mathbf{v}$, points from the target T to the viewer. Effective gaze target position, $\mathbf{T}'$, is the point on $\mathbf{v}$ that is closest to $\mathbf{e_I}$.

Similar to the target pose adaptation techniques described in Section 4.2.1, eye alignment is applied in a view-dependent manner. With low target viewing angles, ϕ_T, the model enforces eye alignment to prevent the viewer from noticing that the character is not actually gazing at them by

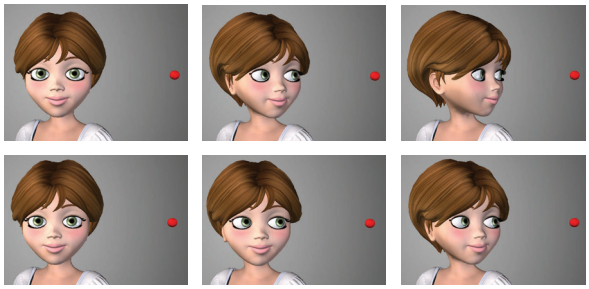

Figure 11: *A performative gaze shift. Top: The character fully aligns with the red sphere. Bottom: The character partially aligns with the target ($\alpha_E = 0.7$) but still appears to be gazing at it, because it has achieved screen-space alignment.*

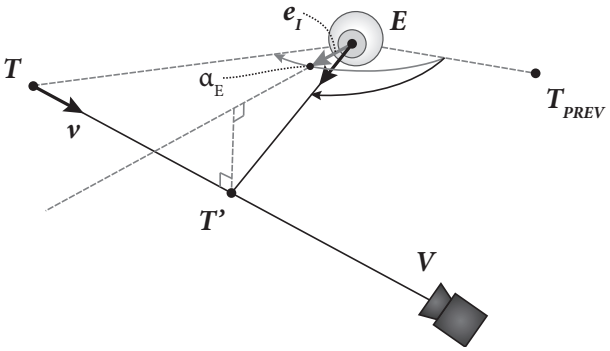

Figure 12: *The calculation of the effective gaze target position in a performative gaze shift.*

automatically adjusting it using the viewing cone parameter, p_ϕ, as follows:

$$\alpha'_E = 1 - p_\phi + \alpha_E p_\phi. \tag{7}$$

5. Evaluation

This section presents two forms of evaluations of our gaze model. The first evaluation involved an *objective* assessment of the effectiveness of our model in reducing the frequency and severity of visual artifacts in gaze shifts on different character designs. The second evaluation followed a human-subjects study and assessed the *perceived* characteristics of the generated gaze behaviors.

5.1. Objective Evaluation

To evaluate the effectiveness of our model in reducing visual artifacts, we have conducted measurements of artifact prevalence on a variety of characters using a set of objective metrics. These metrics reflected the amount of observable artifacts over the course of a gaze shift. Because each artifact is a product of a particular combination of the pose and movement of the eyes and the head, whether or not the artifact is present at a particular frame and its severity can be objectively determined and quantified. Each metric computes the presence of an artifact in each frame and sums them over all the frames of the gaze shift to calculate the "amount" in which the artifact appears. Severity is determined by weighing the amount of an artifact by the cosine fall-off of the viewing angle, ϕ (i.e., angle between view direction and character's gaze direction), thus giving less weight to frames where the character's eyes are less visible. The artifact amount is also weighed by the blink height at each frame to account for eye blinks that partially or fully conceal artifacts. The aggregated amounts are then normalized by the duration of the gaze shift, providing us with quantities that we can compare across different characters and gaze shift configurations. Our metrics include cross-eyedness amount,

© 2013 The Author(s)
© 2013 The Eurographics Association and Blackwell Publishing Ltd.

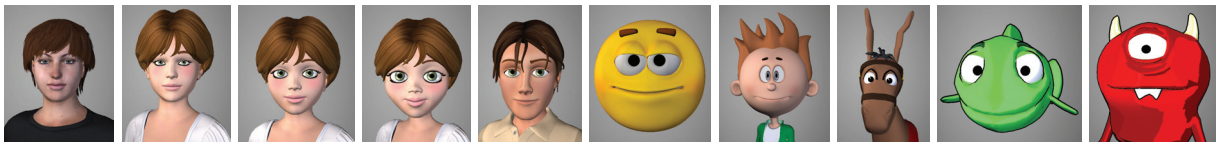

Figure 13: *The characters used in our evaluation. From left to right: RealisticFemale1, RealisticFemale2, SemiStylizedFemale, StylizedFemale, StylizedMale, EmotiGuy, Jack, Donkey, Fish, and NastyMonster.*

τ_{CE}, OMR-block amount, τ_{OMR}, eye retraction and divergence amount, τ_{ERD}, and stuck eye amount, τ_{SE}.

For our test cases, we generated 138 random gaze shifts and applied them to ten different characters, including two with realistic, humanlike proportions (Figure 13). The gaze shifts included an even number of shifts with full and minimal head alignment. For each character, we aggregated the measurements for all gaze shifts with the same head alignment. The results show a reduction in artifact prevalence in almost all test cases as summarized in Table 1 and below:

- Cross-eyedness, τ_{CE}, in characters with human proportions has an average value of 0.30 and goes up to 0.54 in characters with larger inter-eye distances. These levels of cross-eyedness cause unacceptable visual artifacts in stylized characters with large eyes, which are significantly reduced by our model.
- τ_{OMR} is 0.22–0.24 for realistic characters and can be as high as 0.46 in stylized characters with very narrow OMR such as Jack. Our model reduces it by 30–60%, bringing it to about half of normal human levels and achieving a slower movement toward OMR in larger eyes.

Table 1: *Quantitative evaluation results. Each cell contains the aggregate score for a particular metric on a particular character with the baseline model or our proposed model.*

Character	Model	τ_{CE}	τ_{OMR}	τ_{ERD}	τ_{SE}
RealisticFemale1	**Baseline**	0.30	0.24	0.20	0.03
RealisticFemale2	**Baseline**	0.31	0.22	0.20	0.03
SemiStylizedFemale	**Baseline**	0.31	0.23	0.18	0.03
	Proposed	0.07	0.10	0.10	0.02
StylizedFemale	**Baseline**	0.40	0.25	0.21	0.05
	Proposed	0.12	0.10	0.10	0.02
StylizedMale	**Baseline**	0.32	0.22	0.17	0.03
	Proposed	0.09	0.10	0.10	0.03
EmotiGuy	**Baseline**	0.27	0.33	0.20	0.07
	Proposed	0.06	0.12	0.13	0.03
Jack	**Baseline**	0.06	0.46	0.11	0.05
	Proposed	0.07	0.16	0.07	0.06
Donkey	**Baseline**	0.18	0.34	0.22	0.10
	Proposed	0.04	0.10	0.15	0.03
Fish	**Baseline**	0.54	0.30	0.26	0.08
	Proposed	0.16	0.10	0.14	0.03
NastyMonster	**Baseline**	0	0.20	0.29	0
	Proposed	0	0.09	0.18	0

- τ_{ERD} is approximately 0.20, 0.30, and 0.10 in realistic characters, characters with wide (e.g., NastyMonster) or highly asymmetric OMR (e.g., Fish), and characters with low OMR (e.g., Jack), respectively. Our model succeeds in reducing these values by 30–50%.
- Even characters with human proportions exhibit a small amount of stuck eye, τ_{SE}, which we believe is too small to notice. With characters with asymmetric OMR (e.g., EmotiGuy, Jack, Donkey, Fish), τ_{SE} can be as high as 0.10. Our model reduces it to levels seen in human characters. An exception is the Jack character with very narrow OMR, which offers little flexibility in the movement.

5.2. Human Subjects Study

To lessen visual artifacts and afford staging effects, our model deliberately directs the characters's gaze shifts toward locations that are different from the intended gaze targets. While these shifts do not involve geometrically accurate gaze motions, previous studies on gaze perception have shown that people are generally imprecise at judging gaze direction [AC76], suggesting that these deviations might not worsen judgments that already show very high variability. Therefore, the evaluation sought to determine whether these deviations affected the communicative accuracy and perceived naturalness of gaze shifts generated by our model compared with a previously validated baseline model [APMG12b].

Participants – We recruited 48 participants using the Amazon Mechanical Turk crowd-sourcing service. Each participant was paid U.S. $1 for their participation.

Study Design – The study followed a three-by-one, between-participants design. The experimental conditions included gaze shifts performed by (1) *baseline*: a character with human proportions following the baseline gaze model, (2) *baseline stylized*: a character with stylized geometry following the baseline gaze model, and (3) *stylized*: a character with stylized geometry following our gaze model. We chose a between-participants design to minimize transfer effects. Figure 14 illustrates the two characters used in the study. The *stylized* condition involved performative gaze shifts with an eye-alignment parameter of 0.85.

Task – Participants in the study watched a series of videos of the character shifting its gaze toward numbered targets arranged on a whiteboard and tried to identify the target to-

© 2013 The Author(s)
© 2013 The Eurographics Association and Blackwell Publishing Ltd.

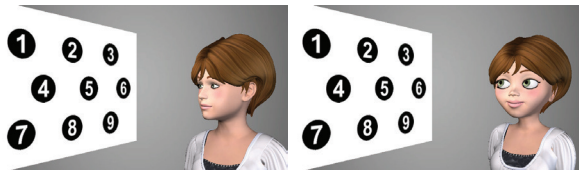

Figure 14: *Stills from videos in our study. Left: Realistically-proportioned character. Right: Stylized character.*

ward which the character was looking (Figure 14). The character was positioned in front of the camera, approximately $1m/3.3ft$ away and slightly to the right. The whiteboard was positioned on the character's right and oriented so that the viewer and the character could comfortably see the targets.

Procedure – After recruitment, each participant reviewed and agreed to a consent form. Following informed consent, the participants viewed a sequence of 22 videos. In each video, the character shifted its gaze toward a randomly selected target from among nine targets on the whiteboard. After watching each video, the participants were asked to determine the target toward which the character was looking and provide their answer in a text field. Each video was approximately ten seconds in length. At the beginning of each video, the character looked toward the camera and nodded. It then shifted its gaze toward one of the targets, maintained its gaze at the target for two seconds, and then looked back toward the viewer.

To ensure the quality of the experimental data, we followed crowd-sourcing best practices [KCS08]. For example, all participants were shown two training and acclimation videos, where the correct gaze target would light up during the gaze shift. Data from participants who failed to correctly identify the target were discarded. We also restricted the task to workers with high approval rates and tracked statistics such as task completion time and screen resolution.

At the end of the study, each participant filled out a questionnaire to provide subjective evaluations of the character. The study took approximately ten minutes.

Measurement & Analysis – The dependent variables in our study were *communicative accuracy*, *naturalness of eye movements*, *lifelikeness*, and *appeal*. Communicative accuracy was measured as the percentage of correctly identified gaze targets. Naturalness of eye movements, lifelikeness, and appeal were measured using a questionnaire. Participants rated each item in the questionnaire using seven-point rating scales ($1 = notlikable$; $7 = likable$). The lifelikeness scale included three items that measured lifelikeness, humanlikeness, and believability ($Cronbach's\alpha = 0.799$), while the appeal scale included four items that measured charisma, attractiveness, cuteness, and likability ($Cronbach's\alpha = .796$).

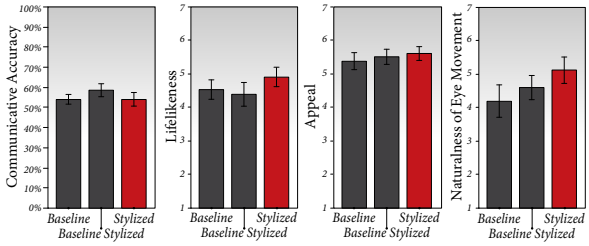

Figure 15: *Results for communicative accuracy, lifelikeness, appeal, and naturalness of eye movements. Data on gaze shifts generated by our model are shown in red.*

Data analysis included one-way analysis of variance (ANOVA) tests, following guidelines suggested by Julnes and Mohr [JM89] for establishing a "no difference" in comparisons, particularly an alpha level of 0.25 (i.e., $p > .25$) to control for Type II errors.

Results – Results for all measures are illustrated in Figure 15. The mean accuracies in the baseline, baseline stylized, and stylized conditions were 54.0%, 58.6%, and 54.0%, respectively. The statistical analysis of the data found no significant effect of our manipulation on accuracy, $F(2,45) = 0.83$, $p = 0.44$. These rates are considerably better than chance, which we expect to be closer to 1/3 than 1/9, as our informal analysis suggests that it is easy to determine toward which row is being looked, and are consistent with results from previous work [AC76, GKC69, APMG12a]. Pairwise contrast tests also found no differences between the baseline and baseline stylized conditions, $F(1,45) = 0.00$, $p = 1.00$, or between the baseline and stylized conditions, $F(1,45) = 1.20$, $p = 0.28$. These results suggest that our model retains the communicative accuracy of the baseline human model.

Our analysis revealed no significant effect of our manipulation on naturalness of eye movements, $F(2,45) = 1.27$, $p = 0.29$. Contrast tests also found no differences between the baseline and baseline stylized conditions, $F(1,45) = 0.53$, $p = 0.47$, or between the baseline and stylized conditions, $F(1,45) = 2.52$, $p = 0.12$, suggesting that our model preserves the naturalness of eye movements generated by the baseline model.

We found no significant effects of our manipulation on the lifelikeness measure, $F(2,45) = 0.69$, $p = 0.51$. Pairwise contrasts showed no differences between the baseline and baseline stylized conditions, $F(1,45) = 0.10$, $p = 0.75$, or baseline stylized and stylized conditions, $F(1,45) = 0.64$, $p = 0.43$. Similarly, we found no effects of our manipulation on the appeal measure, $F(2,45) = 0.25$, $p = 0.78$. No differences appeared in pairwise contrast tests between the baseline and baseline stylized conditions, $F(1,45) = 0.18$, $p = 0.68$, or baseline stylized and stylized conditions, $F(1,45) = 0.49$, $p = 0.49$.

Overall, the results suggest that our gaze model does not change the communicative accuracy and the subjective evaluation of the characters. While we speculate that the removal

© 2013 The Author(s)
© 2013 The Eurographics Association and Blackwell Publishing Ltd.

of artifacts may improve a character's appeal, such effects are unlikely to appear in short, focused tasks. Future studies might further explore how our model shapes subjective impressions of the character in longer, more realistic scenarios.

6. Conclusions

In this paper, we presented a model of gaze shifts that can be applied to a range of characters and provides considerable parametric control. Our model extends a state-of-the-art model of human gaze shifts that achieves the subtle effects seen in natural motions. Our extensions provide significant control over eye geometry and dynamics and allow for view-dependent, performative effects. While the model departs from accurately representing human biological motion, our evaluation confirms that gaze shifts generated by our model are no less accurate or natural than those generated by the baseline model.

The gaze model presented in this paper does not incorporate torso movements, which are simulated in some prior models such as those proposed by Heck [Hec07] and Grillon and Thalmann [GT09]. Moreover, we have not yet explored how our extensions might be applied to other gaze models, although we believe these extensions to be feasible; techniques that modify target pose such as cross-eyedness removal and performative gaze are applicable to any gaze model, as they only require explicit specification of the gaze target. Techniques for gaze dynamics require only the ability to scale the rotational velocity of the eye joints, which is a simple modification in most models.

Our work has also not considered how the parametric model can be used to create high-level effects in real-world applications. For example, Andrist et al. [APMG12b] showed how gaze parameters can be manipulated to improve learning outcomes in an online lecture scenario. We expect that the ability to use stylized, and even non-human, characters will open up further opportunities. Future exploration in this space must also consider communicative cues beyond the gaze shifts explored in this paper. In future work, we plan to continue our exploration of how we can create mechanisms that control aspects of communication for a wide range of characters.

References

[AC76] ARGYLE M., COOK M.: *Gaze and mutual gaze*. Cambridge University Press Cambridge, 1976. 2, 5, 8, 9

[APMG12a] ANDRIST S., PEJSA T., MUTLU B., GLEICHER M.: Designing effective gaze mechanisms for virtual agents. In *Proc. SIGCHI conf. Human factors in computing systems* (2012), CHI '12, ACM, pp. 705–714. 2, 3, 7, 9

[APMG12b] ANDRIST S., PEJSA T., MUTLU B., GLEICHER M.: A head-eye coordination model for animating gaze shifts of virtual characters. In *Proc. 4th Workshop on Eye Gaze in Intelligent Human Machine Interaction: Eye Gaze and Multimodality* (2012). 1, 2, 3, 8, 10

[CE73] CRANACH M. V., ELLGRING J. H.: The perception of looking behaviour. In *Social Communication and Movement*. Academic Press, 1973. 2

[CGV09] CAFARO A., GAITO R., VILHJÁLMSSON H.: Animating idle gaze in public places. In *Proc. 9th intl. conf. Intelligent Virtual Agents* (2009), Springer, pp. 250–256. 2

[DLN05] DENG Z., LEWIS J., NEUMANN U.: Automated eye motion using texture synthesis. *IEEE CG&A* (2005), 24–30. 2

[EMP*94] EVINGER C., MANNING K. A., PELLEGRINI J. J., BASSO M. A., POWERS A. S., SIBONY P. A.: Not looking while leaping: the linkage of blinking and saccadic gaze shifts. *Experimental Brain Research 100* (1994), 337–344. 10.1007/BF00227203. 4

[GB06] GU E., BADLER N. I.: Visual attention and eye gaze during multiparty conversations with distractions. In *Proc. 6th intl. conf. Intelligent Virtual Agents* (Berlin, Heidelberg, 2006), IVA'06, Springer-Verlag, pp. 193–204. 2

[GKC69] GOLDBERG G. N., KIESLER C. A., COLLINS B. E.: Visual behavior and face-to-face distance during interaction. *Sociometry 32*, 1 (1969), pp. 43–53. 2, 9

[GT09] GRILLON H., THALMANN D.: Simulating gaze attention behaviors for crowds. *Comput. Animat. Virtual Worlds 20*, 23 (June 2009), 111–119. 2, 10

[Hec07] HECK R.: *Automated authoring of quality human motion for interactive environments*. PhD thesis, University of Wisconsin–Madison, 2007. 2, 10

[IDP06] ITTI L., DHAVALE N., PIGHIN F.: Photorealistic attention-based gaze animation. In *2006 IEEE Intl. Conf. on Multimedia and Expo* (2006), IEEE, pp. 521–524. 2

[JM89] JULNES G., MOHR L.: Analysis of no-difference findings in evaluation research. *Evaluation Review 13*, 6 (1989), 628–655. 9

[KB01] KHULLAR S., BADLER N.: Where to look? automating attending behaviors of virtual human characters. *Autonomous Agents and Multi-Agent Systems 4*, 1 (2001), 9–23. 2

[KCS08] KITTUR A., CHI E. H., SUH B.: Crowdsourcing user studies with mechanical turk. In *Proc. SIGCHI conf. Human factors in computing systems* (New York, NY, USA, 2008), CHI '08, ACM, pp. 453–456. 9

[LBB02] LEE S., BADLER J., BADLER N.: Eyes alive. In *ACM TOG* (2002), vol. 21, ACM, pp. 637–644. 2

[LM10] LANCE B., MARSELLA S.: The expressive gaze model: Using gaze to express emotion. *IEEE CG&A 30*, 4 (2010), 62–73. 1, 2

[LML09] LI Z., MAO X., LIU L.: Providing expressive eye movement to virtual agents. In *Proc. 2009 intl. conf. Multimodal interfaces* (New York, NY, USA, 2009), ICMI-MLMI '09, ACM, pp. 241–244. 2

[LMT*07] LEE J., MARSELLA S., TRAUM D., GRATCH J., LANCE B.: The rickel gaze model: A window on the mind of a virtual human. In *Proc. 7th intl. conf. Intelligent Virtual Agents* (2007), Springer, pp. 296–303. 2

[PQ10] PETERS C., QURESHI A.: A head movement propensity model for animating gaze shifts and blinks of virtual characters. *Comput. Graph. 34*, 6 (2010), 677–687. 2, 4

© 2013 The Author(s)
© 2013 The Eurographics Association and Blackwell Publishing Ltd.